

Advances in artificial intelligence for the diagnosis and treatment of ovarian cancer (Review)

YANLI WANG^{1*}, WEIHONG LIN^{2*}, XIAOLING ZHUANG³, XIALI WANG⁴,
YIFANG HE¹, LUHONG LI² and GUORONG LYU^{1,4}

Departments of ¹Ultrasound, ²Obstetrics and Gynecology and ³Pathology, The Second Affiliated Hospital of Fujian Medical University; ⁴Department of Clinical Medicine, Quanzhou Medical College, Quanzhou, Fujian 362000, P.R. China

Received July 18, 2023; Accepted January 5, 2024

DOI: 10.3892/or.2024.8705

Abstract. Artificial intelligence (AI) has emerged as a crucial technique for extracting high-throughput information from various sources, including medical images, pathological images, and genomics, transcriptomics, proteomics and metabolomics data. AI has been widely used in the field of diagnosis, for the differentiation of benign and malignant ovarian cancer (OC), and for prognostic assessment, with favorable results. Notably, AI-based radiomics has proven to be a non-invasive, convenient and economical approach, making it an essential asset in a gynecological setting. The present study reviews the application of AI in the diagnosis, differentiation and prognostic assessment of OC. It is suggested that AI-based multi-omics studies have the potential to improve the diagnostic and prognostic predictive ability in patients with OC, thereby facilitating the realization of precision medicine.

Contents

1. Introduction
2. Radiomics
3. AI in the radiomics of OC

Correspondence to: Professor Guorong Lyu, Department of Ultrasound, The Second Affiliated Hospital of Fujian Medical University, 34 North Zhongshan Road, Quanzhou, Fujian 362000, P.R. China

E-mail: lgr_feus@sina.com

Professor Luhong Li, Department of Obstetrics and Gynecology, The Second Affiliated Hospital of Fujian Medical University, 34 North Zhongshan Road, Quanzhou, Fujian 362000, P.R. China

E-mail: liluhong@sina.com

*Contributed equally

Key words: artificial intelligence, radiomics, ovarian cancer, whole-slide imaging

4. Other AI-based omics in OC
5. Conclusions and future perspectives

1. Introduction

Ovarian cancer (OC) is the most common malignancy of the female reproductive system and the fifth leading cause of cancer-associated death in women in the USA (1). In 2020, ~313,956 new cases of OC were diagnosed and ~207,252 OC-associated deaths occurred worldwide (2). Despite therapeutic advances, the responses of patients with advanced OC remain unsatisfactory, with 70% of patients experiencing relapse after treatment. Consequently, the survival rate is extremely low, making OC one of the primary causes of cancer-associated mortality in women (3). In 2020, the number of OC-associated deaths in the USA reached 13,438, accounting for 4.2% of all cancer-related deaths (1).

Histopathologically, 90% of all OC develops from epithelial cells, and the main subtypes are serous and mucinous (4). The World Health Organization (WHO) previously published a classification standard for tumors of the female genital organs, which categorizes epithelial OC (EOC) into two types based on the genetic lineage (5). Type I EOC includes low-grade serous carcinoma, low-grade endometrioid carcinoma, clear cell carcinoma and mucinous carcinoma. Type I EOCs develop from benign or borderline ovarian lesions and are characterized by slow growth, being typically confined to the ovaries and exhibiting large unilateral cystic tumors (6,7). The genetic mutations in type I EOCs are more stable, such as KRAS, BRAF, CTNNB1, PTEN, PIK3CA, ARID1A, and PPP2R1A and ERBB2 mutations, while the TP53 mutation is rare (8). Surgery is an effective treatment for early stage type I EOCs, but advanced cases are often unresponsive to cytotoxic chemotherapy, with targeted drugs, such as BRAF inhibitors, showing some efficacy. Type II EOC includes high-grade serous carcinoma, high-grade endometrioid carcinoma, carcinosarcoma and undifferentiated carcinoma (9). Most patients are diagnosed in the first instance with advanced-stage cancer, exhibiting invasion of extra-ovarian tissues, although type II EOCs usually present as small lesions involving both ovaries. Furthermore, the tumor volume at the site of metastasis is

large, accompanied by ascites and other malignant tumor signs. TP53 mutations and CCNE1 amplification are present in >80% of patients with type II EOC, while other mutations are rare (10). Although traditional platinum-based chemotherapy is effective for the majority of type II EOCs, the overall survival (OS) rate of patients remains poor due to a high propensity for relapse (11). In summary, the prognosis of patients with type I EOCs is generally more favorable than those with type II EOCs (12).

Artificial intelligence (AI), a branch of computer science, refers to the ability of computer systems to learn from input data. AI is playing an important role in areas of medical research, including imaging, pathomics, genomics, transcriptomics, proteomics and metabolomics. In recent years, AI-based multi-omics research has been widely conducted with a focus on OC diagnosis, benign and malignant differentiation, and the prediction of pathological classification, drug efficacy and prognosis. Researchers have studied and reviewed the clinical application of AI in OC. Shrestha *et al* (13) reviewed AI methods, imaging methods and clinical parameters in gynecological tumors, such as endometrial cancer, cervical cancer and OC. However, this previous study is limited to only discussing the content based on medical images, and there is no elaboration on other omics-based technologies, such as pathomics, genomics, transcriptomics and several other omics. Similarly, Mikdadi *et al* (14) reviewed the use of AI in the diagnosis and prognosis of OC and pancreatic cancer; however, the study did not provide detailed research progress of AI in various other omics-based approaches (14). In addition, Shrestha *et al* (13) reviewed the application of AI for the processing of medical images, clinical information and biological information of common gynecological tumors. Breen *et al* (15) reviewed studies on the use of AI for the analysis of histopathological images in OC, and evaluated the role of various AI models in the diagnosis and prognosis of the disease. Notably, most of the aforementioned studies are limited to evaluating the application value of uniomics in AI. In the present study, a comprehensive review of the workflow of AI and its applications in imaging, pathomics, genomics, transcriptomics, proteomics and metabolomics is provided.

2. Radiomics

Radiomics is a non-invasive approach to extract high-throughput imaging features from the medical images of techniques such as computed tomography (CT), magnetic resonance imaging (MRI) and ultrasound, and was first proposed by Lambin *et al* in 2012 (16). Medical images contain high-throughput digital information related to tumor pathophysiology (17). Moreover, radiomics can be used to extract relevant features from images, and combine and supplement the findings with clinical information, pathophysiology and molecular biological information, so as to improve clinical diagnosis, predict the tumor stage and genotype, and assess the prognosis (18,19). The major steps of radiomics include medical image acquisition, image segmentation, feature extraction, feature screening and model building (Fig. 1). Radiomics has been widely used in the research of various tumors, including thyroid (20), breast (21), liver (22) and prostate (23) cancer, and OC (24).

Image acquisition. CT, MRI, positron emission tomography (PET) and ultrasound are the most common image acquisition methods (25). Images obtained by the same machine equipment, scanning method and scanning layer thickness need not undergo post-processing during feature extraction. However, images obtained using different equipment and acquisition conditions require pre-processing before feature extraction. The pre-processing process includes resampling, standardization and high-pass filtering, to obtain a uniform layer thickness and matrix size for feature extraction. Due to the limitations of imaging conditions imposed by radiomics, there are few prospective studies (26). Most research has been conducted as retrospective studies (20-24), thus the medical images acquired come from hospital image storage systems or online databases (27).

Image segmentation. After obtaining medical images, a region of interest (ROI) is typically delineated, which involves automatic segmentation, manual segmentation and semi-automatic segmentation. Automatic segmentation is fast in delineating lesions, but poor in identifying them. In addition, the edge of tumors on most medical images is vague, and the influence of surrounding metastases and accompanying symptoms, such as inflammation, on the image easily interferes with the contours created by semi-automatic and automatic segmentation. Manual segmentation, on the other hand, is subjective and slow, as it depends on the identification of the lesions and drawing of contours by clinicians. Semi-automatic segmentation, based on automatic segmentation, allows clinicians to 'proofread' the delineated edges manually, which can improve the efficiency and accuracy of the delineation (28). Currently, ordinary ROI mapping software includes MIM (www.mimsoftware.com), ITK-SNAP (www.itksnap.com), 3DSlicer (www.slicer.org) and ImageJ (National Institutes of Health) software.

Feature extraction. Radiomics features include the morphological, first-order, second-order and higher-order features of the tumor itself (29). Morphological features include the tumor shape, size, vascular distribution and its relationship with surrounding tissue, amongst other features. However, each feature alone provides general characteristics of the tumor instead of tumor heterogeneity. First-order features are also recognized as intensity features, which are related to the distribution of gray-level intensities in the ROI. The histogram represents the number of pixels with a certain gray level in the image, reflecting the frequency of each gray level in the image. Information such as maximum, minimum, mean, mean absolute deviation, median, skewness, standard deviation, consistency, variance, energy and entropy can be obtained from the intensity histogram. The second-order features include the gray co-occurrence matrix and the gray run length matrix, which can estimate the spatial distribution relationship of the image gray value. The higher-order features include the neighborhood gray difference matrix and gray region size matrix. The gray difference matrix of the neighborhood can evaluate the pixel heterogeneity between the ROI and adjacent regions, while the gray region size matrix can evaluate the characteristics of homogeneous regions (30).

Feature screening. In the process of feature extraction, several features will be identified, which may lead to overfitting when

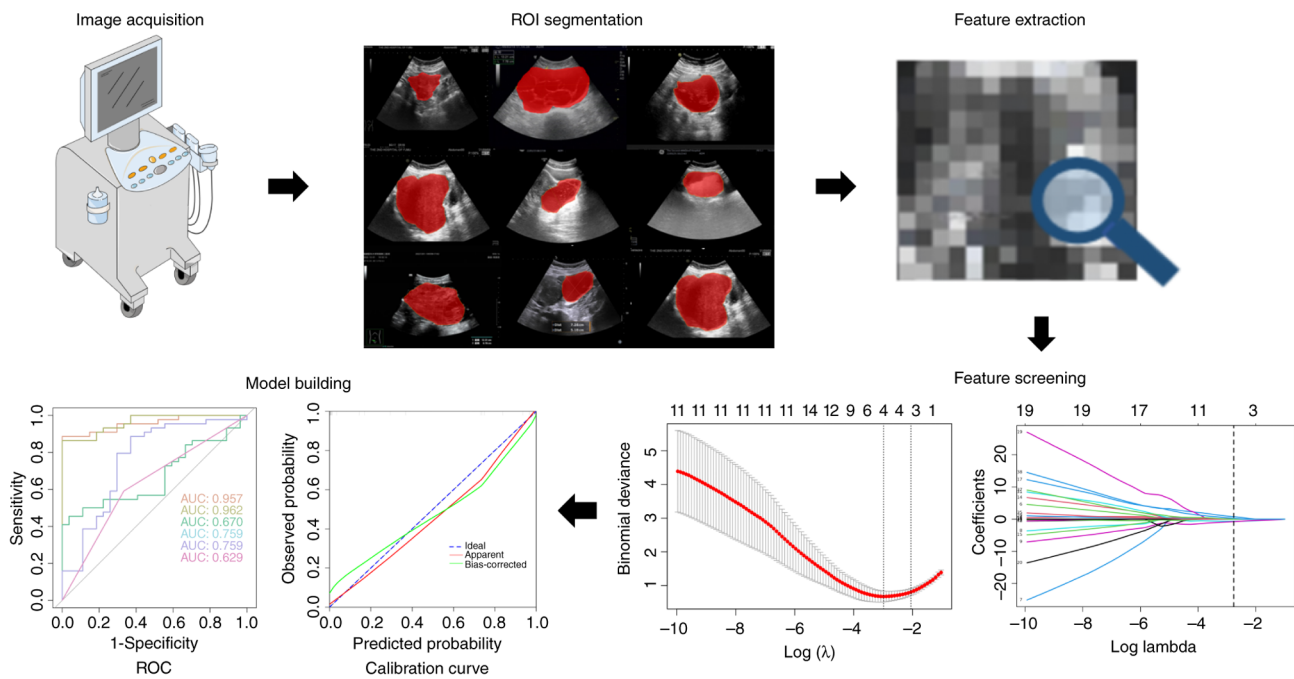


Figure 1. Flow chart of radiomics. The process of radiomics includes image acquisition, ROI segmentation, feature extraction, feature screening and model building. ROC and calibration curves are often used to evaluate the model performance in the process of model building. ROI, region of interest; ROC, receiver operating characteristic. The statistical images (feature screening and model building) are from Dr Yanli Wang (unpublished data).

the data set is smaller than the feature set (31). To avoid this overfitting of the model, several features must be selected. Feature screening is usually achieved using AI or statistical methods, and commonly used methods include maximum correlation minimum redundancy, principal component analysis and least absolute shrinkage and selection operator (LASSO) regression, amongst other approaches (32).

Model building. The final step in radiomics is the establishment of the model, which can combine patient clinical data, susceptibility factors and biomarkers with radiomics to create a more precise model. For example, a nomogram is often used in the modeling of imaging omics (33). The establishment of these models has improved the ability of clinicians to diagnose and differentiate diseases. Some models can also predict pathological types and patient outcomes, which contributes to the implementation of personalized medicine and modern medicine. Several studies have combined imaging with genomics, transcriptomics, proteomics and metabolomics to build diagnostic models, gene expression models and prognostic models of diseases (34-36).

3. AI in the radiomics of OC

Traditional imaging diagnosis relies on a clinician's subjective judgment of the visual information (37). However, AI can standardize and simplify the process by extracting the available information from the images by mimicking the cognitive behaviors associated with the human brain (38). Therefore, AI can be applied to the process of feature screening and model building in radiomics. The significant differences in AI diagnostics using imaging depend on who created the AI model (39). AI includes machine learning (ML), significant

data management and information mining, image processing and pattern recognition. ML is the approach and core of medical AI, including supervised learning, unsupervised learning and reinforcement learning (40,41). Supervised learning refers to the application of known cohorts as known information of learning, so as to build a classification and prediction model for unknown cohorts (42). However, the data results are not necessary for the construction of the unsupervised learning model, and the data can be summarized and classified (43). Reinforcement learning is a computational method to understand and automatically process goal-oriented learning and decision-making problems, and there are several advantages, such as direct interaction with the environment and autonomous learning without the need for emulated supervisory signals for modeling (44). Notably, ML is an essential branch of AI, and the major procedures include data collection and processing, model training and optimization, and model evaluation, amongst others (45). ML can establish models by converting medical images into features or labels and subsequently performing a mapping from features to labels using algorithms. ML primarily includes logistic regression, artificial neural networks (ANNs), support vector machines and deep learning convolutional neural networks (DCNNs) (46). Deep learning (DL) is a subset of ML, which can use multiple ANNs to solve complex problems based on the structure of brain neurons. Neural networks can link dependent and independent variables together without prior knowledge to detect patterns and nonlinear interactions in complex data (47). CNNs, a subset of AI and DL, are a special type of computational model the principle of which is to imitate neurons and synapses in the human brain (Fig. 2) (47). A neural network with more hidden layers is defined as a deep neural network. DL can solve various classification and prediction problems using

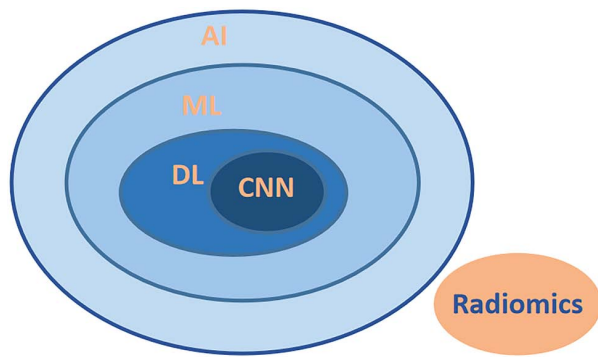


Figure 2. Relationship of the AI algorithm. The internal inclusion relationship of the AI algorithm, and the paratactic relationship with radiomics. AI, artificial intelligence; ML, machine learning; DL, deep learning; CNN, convolutional neural network.

deep neural networks; it can also identify features from data automatically and avoiding manual feature selection, which is an apparent advantage compared with traditional ML (48).

Radiomics, ML and DL are not independent individuals, but are intricately intertwined for the most part. The modeling process in radiomics usually relies on DL (49). AI has been widely used in the diagnosis of diseases, the differentiation of benign and malignant tumors, and the prediction of therapeutic effects (50) (Fig. 3).

Identification of benign and malignant tumors. The comprehensive evaluation of ovarian tumors, both benign and malignant, requires a preliminary judgment by clinicians based on symptoms, and laboratory and imaging examinations. At present, the gold standard for determining benign and malignant ovarian tumors is still pathological analysis of a puncture biopsy or postoperative pathological examination. However, the methods are invasive, and puncture biopsy carries a certain risk of needle path metastasis (51). Therefore, a number of studies have explored the application of radiomics in the identification of benign and malignant tumors. For example, Wang *et al* (52) retrospectively collected CT images of patients with EOC from multiple centers to establish a CT radiomics model that could distinguish high-grade serous OC (HGSOC). The areas under the curve (AUCs) were 0.837 (95% CI, 0.835-0.838) for the training cohort and 0.836 (95% CI, 0.833-0.840) for the testing cohort. The study confirmed that the radiomics model is important for the individualized treatment and prognostic evaluation of patients. Similarly, Li *et al* (53) reported the effectiveness of radiomics. This previous study established a radiomics model to identify benign and malignant ovarian tumors based on 143 CT images. The AUCs for both the training set (0.88) and the test set (0.87) were high, which confirmed the discriminative ability of the model. A nomogram combining clinical information and serum markers was also created. Saida *et al* (54) reported that the established CNN model of OC diagnosis based on MRI also showed a good diagnostic effect. Moreover, it was demonstrated that the differential model based on radiomics had a higher average diagnostic efficiency than the radiologist (internal data set: 88.8 vs. 85.7%; external validation data set: 86.9 vs. 81.1%), and the combined use of the model could improve the efficiency of the radiologist. The accuracy [87.6% (95% CI, 85.0-90.2) vs.

78.3% (95% CI, 72.1-84.5); $P<0.0001$] and sensitivity [82.7% (95% CI, 78.5-86.9) vs. 70.4% (95% CI, 59.1-81.7); $P<0.0001$] of DCNN-assisted diagnosis were higher than the values for the radiologists alone (55). Wang *et al* (56) also explored the MRI of 201 patients with borderline ovarian tumors and 99 patients with EOC, and established a differential diagnosis model based on DL. The results revealed that the accuracy of the AI model was higher than that of the radiologists. A recent study showed that the models based on DL had an AUC of 0.93 (95% CI, 0.85-0.97) for differentiating malignant from benign ovarian tumors, which was comparable with the Ovarian-Adnexal Reporting and Data System (O-RADS) (57) (AUC, 0.92; 95% CI, 0.85-0.97; $P=0.88$) and expert assessment (AUC, 0.97; 95% CI, 0.91-0.99; $P=0.07$) (58). The models based on DL decision, DL feature, O-RADS and expert assessment achieved sensitivities of 92, 92, 92 and 96%, respectively, and specificities of 80, 85, 89 and 87%, respectively, for malignancy. Therefore, the models based on DL may distinguish malignant from benign ovarian tumors with a diagnostic performance comparable to expert subjective and Ovarian-Adnexal Reporting and Data System assessment. In addition, the specificity and sensitivity of the models established by different AI algorithms for the identification of ovarian tumors are also different (58). Other researchers have also shown that AI models based on ultrasonic images have high accuracy and sensitivity for the identification of OC, and the differentiation of benign and malignant tumors. Furthermore, the diagnostic efficacy is similar to that of ultrasound experts (59,60).

Pathological classification. EOC is classified into type I and type II according to the classification standard of female reproductive organ cancers from the WHO in 2014 (61). Due to the difference in treatment and prognosis between type I and type II EOC, it is necessary to classify the pathological type after a diagnosis of OC (5). In this regard, Tang *et al* (62) investigated ultrasonic images of patients with EOC ($n=154$), and divided them into type I and type II EOC according to the pathology. The seven features with the greatest differences were screened out using LASSO regression ten-fold cross-validation. As a result, an identifiable model was established with satisfactory predictive efficiency, with AUCs of 0.817 and 0.731 for the training and test sets, respectively. Furthermore, radiomics can be utilized to evaluate tumor heterogeneity in addition to predicting pathological types. Xu *et al* (63) analyzed the MRI results of patients with EOC ($n=146$), and established a model and nomograms for distinguishing EOC from borderline ovarian tumors and EOC subtypes using logistic regression. The study mapped not only the solid components of the tumor tissue, but also the overall region of the tumor tissue, providing a more complete evaluation of the tumor heterogeneity. Jian *et al* (64) conducted a multicenter retrospective analysis of MRI results in patients with EOC ($n=294$) and established a radiomics model that distinguished type I from type II by extracting relevant radiomics features from axial sequences of T2-weighted images with fat saturation (T2WIFS), diffusion-weighted imaging (DWI), apparent diffusion coefficient and contrast enhanced (CE)-T1WI. The model showed good diagnostic performance in both internal and external validation cohorts, with AUCs of 0.806 and 0.847, respectively. Additionally, an occlusion experiment was

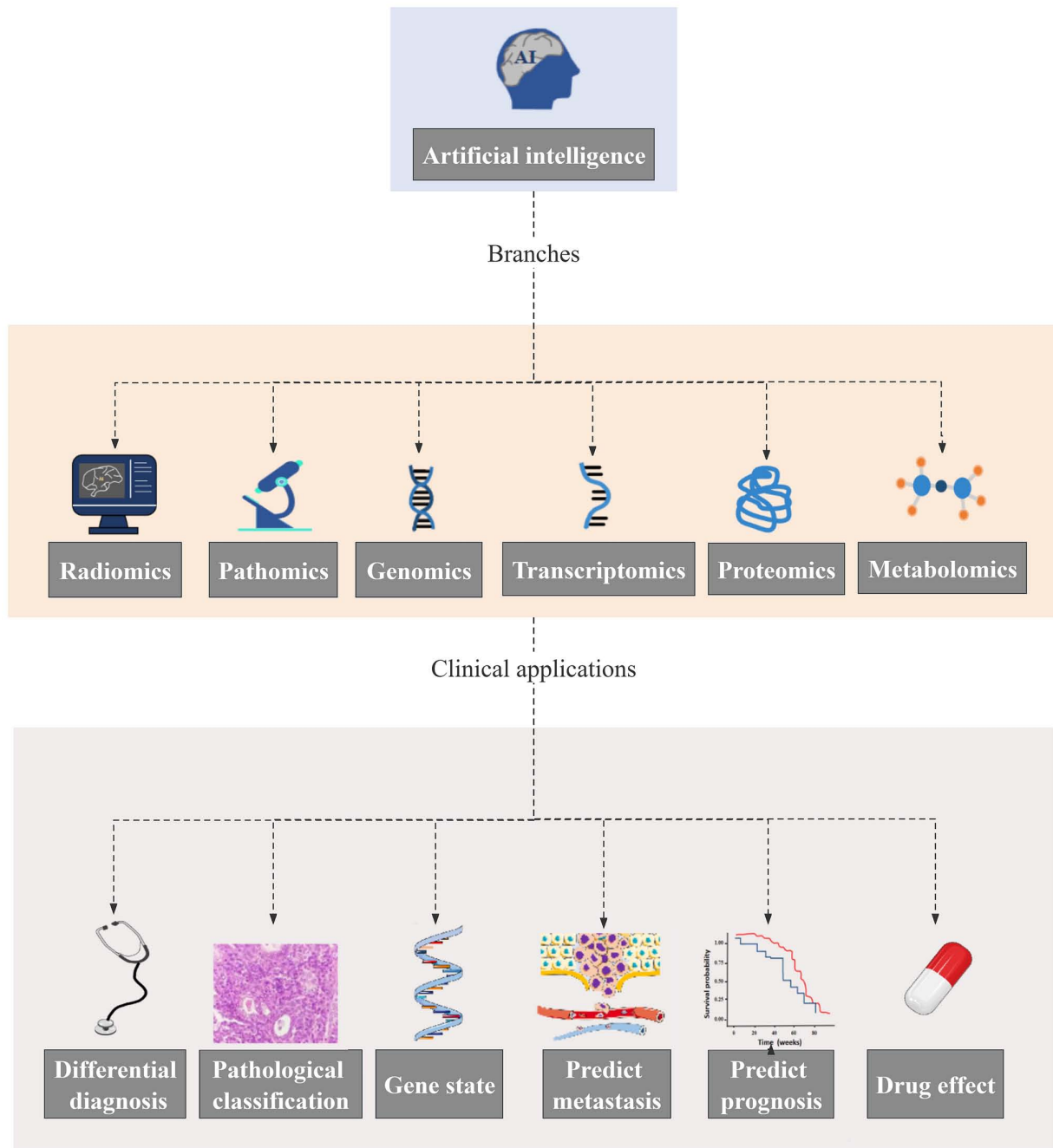


Figure 3. AI in omics. AI is widely used in radiomics, pathomics, genomics, transcriptomics, proteomics and metabolomics. These omics can be used in a number of clinical applications, including differential diagnosis, pathological classification, predicting gene state, tumor metastasis, prognosis and drug response.

conducted to locate the critical areas of the image for model building and diagnosis. The results showed that the most important area used to identify type I and type II EOCs was located at the junction between solid and cystic components, and in the area with a low density of solid components in T2WIFS. This conclusion may provide a basis and guidance for puncture diagnosis of tumors and pathological sampling.

Gene mutation state. Studies have demonstrated that ~50% of EOC cases carry homologous recombination repair defects, which are primarily caused by mutations in the breast cancer susceptibility gene (BRCA). BRCA can participate in the repair of DNA double-strand breaks during the

process of homologous recombination repair, and is a crucial tumor suppressor gene (65,66). Patients with advanced OC accompanied by BRCA mutations are more responsive to platinum-based chemotherapy drugs, exhibiting higher objective response rates and survival rates (66-69). The 5-year survival rate and progression-free survival (PFS) rates of patients with BRCA mutation-positive OC are higher than those without mutations (70). Moreover, BRCA1/2 mutation-positive patients have also shown good reactivity when treated with platinum-based agents in patients with a recurrent case of OC (71). Therefore, it is essential to make a definitive diagnosis of any BRCA mutations before treatment in order to aid the clinical planning and evaluation of a

patient's prognosis. Current guidelines from different scientific societies also recommend the genetic testing of BRCA1/2 for newly diagnosed patients with a non-mucinous EOC (72). Although puncture sampling is commonly used to detect BRCA gene status in patients, it is an invasive method that may cause cancer cell metastasis along the puncture needle tract during the process. Furthermore, the gene expression within tumors may have certain heterogeneity (73), and the puncture sampling method can only perform genetic identification on some of the tissues, instead of evaluating the overall genetic diversity of the entire tumor (74). Additionally, genetic testing is costly and time-consuming (75). Radiomics has emerged as a promising alternative to genetic testing in recent years. A number of studies have applied radiomics to assess the gene state of OC. Meier *et al* (73) retrospectively collected the CT images from 88 patients with HGSOC, and extracted the texture features. The results showed that the radiomics features were significantly correlated with the prognosis of the patients, but not with the status of BRCA mutations, which may be due to the small number of patients assessed. In addition to BRCA, Ki-67 was also significantly correlated with the recurrence and prognosis of OC. Wang *et al* (76) analyzed the PET/CT images of patients with HGSOC ($n=161$). The radiomics features of the whole tumor area were extracted based on a Habitat method and a model for predicting the Ki-67 status of OC was established. The results verified that radiomics could predict the expression of Ki-67 accurately and might be a novel marker to replace Ki-67. Additionally, the Habitat model could stratify prognosis more efficiently ($P<0.05$).

Metastasis. Advanced OC is typically accompanied by intra-abdominal diffusion and distant metastasis at first diagnosis. It has been shown that the 5-year survival rate of patients with OC is only 20-45% (77). Therefore, it is essential to detect metastases early, as this affects the treatment used and the management from stage to stage. However, the positive rate for detection of small metastases by conventional means remains poor (78). A novel approach, radiomics, has been shown to predict metastasis more accurately (79). Ai *et al* (80) explored the CT images of patients with OC ($n=101$), and identified nine radiomic features for screening from a total of 184. The results revealed that the radiomics model and the comprehensive model combined with age and cancer antigen 125 levels could be used to predict the metastatic status. Similarly, MRI-based research has validated the role of radiomics in predicting OC metastasis. Yu *et al* (81) established a nomogram for predicting peritoneal metastasis based on radiomics characteristics and clinical data from FS-T2WI, DWI and dynamic CE-MRI images of 86 patients with OC. The comprehensive nomogram (AUC, 0.902) combining radiomics characteristics and clinicopathological risk factors showed a better diagnostic effect than the clinical model (AUC, 0.858) and the radiomics model (AUC, 0.846). These findings suggest that the radiomics model is a promising method for predicting OC metastasis, particularly small metastases, and may thus be used to improve the detection rate.

Postoperative residue and prognosis. In total, >70% of patients with OC are diagnosed at an advanced stage (82), and the current standard treatment involves initial tumor cell reduction

and platinum-based chemotherapy. However, the effectiveness of initial tumor cell reduction and patient response to chemotherapy drugs vary due to individual differences (such as gene mutation status and physiological status) and tumor heterogeneity. Therefore, it is important to predict a patient's response before and after treatment (83). Radiomics has emerged as a promising tool for predicting the postoperative tumor residual status of patients and the risk of recurrence after receiving chemotherapy drugs, which will be conducive to the selection of chemotherapeutic drugs, chemotherapeutic methods and the formulation of individualized follow-up periods (84). Lu *et al* (85) applied ML to obtain the radiomic prognostic vector (RPV) for 364 patients with EOC. It was reported that RPV could be used to assess patient outcomes in discovery datasets, which was well validated in validation datasets and the Cancer Genome Atlas validation dataset. Meier *et al* (73) extracted CT features from pre-treatment images of 88 patients with HGSOC and found that these features were relevant to patient PFS and OS time. A study by Hong *et al* (86) also verified the ability of a model to predict OS in patients with OC. CT images of serous OC were selected from the cancer imaging archive as the model training set, while images collected in the study hospital were used as the validation set, and three radiomics features were finally screened out. Furthermore, the nomogram, in combination with clinical data, was established as a model to evaluate the OS with serous OC, which will be helpful for the formulation of treatment strategies and the prognostic evaluation of patients. Wei *et al* (87) verified the relationship between PFS and the radiomics characteristics of advanced HGSOC through Kaplan-Meier survival analysis and a Cox proportional risk model, and established a nomogram for predicting the recurrence risk of HGSOC. Notably, not only did the model have a good predictive effect, but other DL models based on MRI and CT images did also (88,89). Compared with CT and MRI, ultrasound is more convenient and economical. In recent years, ultrasonography has been used to establish a prognostic model for OC. In one study, 111 patients with EOC were examined by transvaginal ultrasonography, and the characteristics of ultrasonography were extracted to establish a comprehensive PFS prediction model combined with clinical variables (90). Additionally, AI can predict the length of postoperative hospital stay for patients with HGSOC (91), which may contribute to the individualized treatment and management plans in clinical practice.

Response to chemotherapy. Lei *et al* (92) included MRI (CE-T1WI and T2WI) of 93 patients with EOC who had received platinum-based chemotherapy (≥ 4 cycles), and established two different models based on the primary tumor or the entire abdomen as areas of interest. Furthermore, 1,024 features were extracted using the pre-trained CNN model. The results showed that the whole abdominal DL model based on MRI was effective in predicting the sensitivity of patients with EOC to platinum-based therapy (Table I).

Identification of whole slide images based on DL. A pathological biopsy is the gold standard for diagnosing EOC, and it is also a mandatory examination mode during postoperative chemotherapy in patients with advanced OC. The clinician can make a more individualized treatment plan for the patient

Table I. Overview of the studies on AI in radiomics.

| A, Identification of benign and malignant tumors | | | | | | | |
|--|----------|--------------------|-----------------|----------|---|--|---------|
| First author, year | Disease | Number of patients | Type of imaging | AI model | Main result | Main conclusion | (Refs.) |
| Wang <i>et al</i> , 2022 | EOC | 665 | CT | LR | The AUCs of the LR model in differentiating high-grade serous carcinoma and non-high-grade serous carcinoma were 0.837 (95% CI, 0.835-0.838) for the training cohort and 0.836 (95% CI, 0.833-0.840) for the testing cohort. | Radiomic features extracted from contrast-enhanced CT are useful in the classification of histological subtypes in EOC. | (52) |
| Li <i>et al</i> , 2021 | OC | 134 | CT | DL | The AUC in the training set was 0.88 and the AUC in the test set was 0.87. | The model based on CT images is helpful for the identification and prediction of benign and malignant ovarian neoplasms. | (53) |
| Saida <i>et al</i> , 2022 | OC, BOT | 146 | MRI | CNN | The sensitivity, specificity, accuracy and AUC of CNN were 0.77-0.85, 0.77-0.92, 0.81-0.87 and 0.83-0.89, respectively. The CNN showed the highest diagnostic performance on the ADC map among all sequences (specificity, 0.85; sensitivity, 0.77; accuracy, 0.81; AUC, 0.89). | CNNs exhibit a diagnostic performance that is non-inferior to that of radiologists. | (54) |
| Gao <i>et al</i> , 2022 | OC | 3,755 | US | CNN | Accuracy and sensitivity of diagnosis increased more after DCNN-assisted diagnosis than after assessment by radiologists alone [87.6% (85.0-90.2) vs. 78.3% (72.1-84.5), P<0.0001; 82.7% (78.5-86.9) vs. 70.4% (59.1-81.7), P<0.0001]. | The performance of the CNN model exceeds the average diagnostic level of the radiologist and can enhance the accuracy of the radiologist. | (55) |
| Wang <i>et al</i> , 2023 | EOC, BOT | 102 +99 | MRI | DL | The DL model could differentiate BOT from EOC with a higher AUC of 0.87, an accuracy of 83.7%, a sensitivity of 75.0% and a specificity of 87.5%. | The DL model based on MRI can distinguish BOT from EOC accurately, which is superior to radiologists. | (56) |
| Jung <i>et al</i> , 2022 | OC | 1,154 | US | CNN | The accuracy of the CNN model was 97.2%, the sensitivity was 97.2% and the AUC was 0.9936 in terms of distinguishing normal and ovarian tumors. The CNN model showed 90.12% accuracy, 86.67% sensitivity and 0.9406 AUC in distinguishing malignant ovarian tumors. | The CNN model can recognize valid texture and morphology features from the US images and classifies ovarian tumors. | (59) |
| Christiansen <i>et al</i> , 2021 | OC | 758 | US | CNN | At a sensitivity of 96.0%, model 1 had a specificity similar to that of subjective assessment (86.7% vs. 88.0%; P>0.999). Model 2 had a sensitivity of 97.1% and a specificity of 93.7% when designating 12.7% of the lesions as inconclusive. | CNN models can predict ovarian malignancy accurately, comparable to the human results, which demonstrates that the models are crucial in the triage of ovarian tumors. | (60) |

Table I. Continued.

| B, Pathological classification | | | | | | |
|--------------------------------|---------|--------------------|-----------------|------------------|--|--|
| First author, year | Disease | Number of patients | Type of imaging | AI model | Main result | Main conclusion (Refs.) |
| Tang <i>et al</i> , 2022 | EOC | 154 | US | ML | The AUCs of the training set and test set in the radiomics model and comprehensive model were 0.817 and 0.731, and 0.982 and 0.886, respectively. | The radiomics model based on ultrasound has a great predictive effect for differentiating type I and type II EOC. (62) |
| Xu <i>et al</i> , 2022 | EOT | 146 | MRI | LR | The radiomics model showed more favorable discrimination than the clinical model (0.915 vs. 0.852, and 0.954 vs. 0.852, respectively) in distinguishing BOT from EOC in the training cohort. The radiomics model was superior to the clinical model (AUC 0.905 vs. 0.735) in classifying early stage type I and type II EOC. | Radiomics based on DWI is an effective approach to categorize EOTs. (63) |
| Jian <i>et al</i> , 2021 | EOC | 294 | MRI | LASSO | The combined radiomics model was superior to the single-parametric radiomics models in internal and external validation cohorts (AUCs of 0.806 and 0.847, respectively). | The radiomics model based on MRI can differentiate type I and type II EOC. (64) |
| Meier <i>et al</i> , 2019 | HGSOC | 88 | CT | GLCM | Higher values of all three metrics were significantly associated with lower complete surgical resection status in BRCA-negative patients (SE, $P=0.039$; SCV, $P=0.006$; SCP, $P=0.02$), but not in BRCA-positive patients (SE, $P=0.7$; SCV, $P=0.91$; SCP, $P=0.67$) | The radiomics model based on CT is an important tool to predict the outcome. (73) |
| Wang <i>et al</i> , 2022 | HGSOC | 161 | PET/CT | Habitat | The texture features generated by the Habitat could predict the Ki-67 state, which is more efficient than the texture features extracted from the whole tumor ($P<0.001$). | This model can guide the stratification of prognosis in patients with HGSOC and is related to the expression of Ki-67 in tumor tissues. (76) |
| C, Metastasis | | | | | | |
| First author, year | Disease | Number of patients | Type of imaging | AI model | Main result | Main conclusion (Refs.) |
| Ai <i>et al</i> , 2021 | OC | 101 | CT | Ridge Regression | The AUCs of the radiomics model, clinical model and combined model were 0.82 (95% CI, 0.66-0.98; sensitivity, 0.90; specificity, 0.70), 0.83 (95% CI, 0.67-0.95; sensitivity, 0.71; specificity, 0.8) and 0.86 (95% CI, 0.72-0.99; sensitivity, 0.81; specificity, 0.8), respectively. | Radiomics model can predict the metastatic status for patients with OC. (80) |

Table I. Continued.

| C, Metastasis | | | | | |
|--|---------|--------------------|-----------------|----------|---|
| First author, year | Disease | Number of patients | Type of imaging | AI model | Main result |
| Yu <i>et al</i> , 2021 | OC | 86 | MRI | LR | The nomogram (AUC, 0.902) constructed by combining radiomics characteristics and clinicopathological risk factors showed a better diagnostic effect than the clinical model (AUC, 0.858) and the radiomics model (AUC, 0.846). |
| | | | | | Main conclusion |
| | | | | | Radiomics nomogram based on MRI has a good predictive accuracy for patients with OC. |
| | | | | | (Refs.) |
| | | | | | (81) |
| D, Postoperative residue and prognosis | | | | | |
| First author, year | Disease | Number of patients | Type of imaging | AI model | Main result |
| Lu <i>et al</i> , 2019 | EOC | 364 | CT | ML | RPV remained significantly and continuously associated with OS in the discovery dataset (HR, 3.83; 95% CI, 2.27-6.46; $P=5.11 \times 10^{-7}$; RPV range, -0.322 to 3.16), as well as TCGA validation dataset (HR, 4.87; 95% CI, 1.67-14.2; $P=0.0038$) and the HH validation dataset (HR, 7.36; 95% CI, 1.29-41.9; $P=0.0245$). |
| Meier <i>et al</i> , 2019 | HGSOC | 88 | CT | GLCM | Higher SCV was associated with lower PFS ($P=0.006$) and OS ($P=0.003$). Higher SCP was associated with lower PFS ($P=0.02$) and higher SE was correlated with lower OS ($P=0.01$). |
| Hong <i>et al</i> , 2022 | HGSOC | 119 | CT | LASSO | The nomogram showed great discrimination in the training set (C-index, 0.754; 95% CI, 0.678-0.830), which was confirmed in the validation set (C-index, 0.727; 95% CI, 0.569-0.885). |
| Wei <i>et al</i> , 2019 | HGSOC | 142 | CT | LASSO | The accuracy values of radiomic nomogram for predicting 18-month and 3-year recurrence risks were 84.1% (95% CI, 80.5-87.7%) and 88.9% (95% CI, 85.8-92.5%), respectively. |
| Wang <i>et al</i> , 2019 | HGSOC | 245 | CT | DL | Two patient groups with high and low recurrence risk ($P=0.0038$ and $P=0.0164$) could be clearly identified by Kaplan-Meier analysis. The 3-year recurrence prediction was also effective (AUC, 0.772 and 0.825, respectively). |
| | | | | | Main conclusion |
| | | | | | RPV and the associated analysis platform could be exploited to guide personalized therapy of EOC. |
| | | | | | (Refs.) |
| | | | | | (85) |
| | | | | | The features are relevant to the patient PFS and OS. |
| | | | | | (73) |
| | | | | | The radiomic-clinical nomogram can increase the predictive accuracy of OS in patients with HGSOC after surgery. |
| | | | | | (86) |
| | | | | | Radiomic signature is a potential prognostic marker, which can be used to evaluate the patients with advanced HGSOC. |
| | | | | | (87) |
| | | | | | The DL model based on CT can predict the prognosis of patients with HGSOC. |
| | | | | | (88) |

D, Postoperative residue and prognosis

AI, artificial intelligence; OC, ovarian cancer; EOC, epithelial ovarian cancer; CT, computed tomography; LR, logistic regression model; DL, deep learning; MRI, magnetic resonance imaging; CNN, convolutional neural network; US, ultrasound; ML, machine learning; BOT, borderline ovarian tumor; EOT, epithelial ovarian tumors; LASSO, least absolute shrinkage and selection operator; SE, inter-site cluster variance; SCP, inter-site cluster prominence; GLCM, gray-level co-occurrence matrix; HGSOc, high-grade serous ovarian cancer; AUC, area under the curve; ADC, apparent diffusion coefficient; HH, Hammersmith Hospital; DCNN, deep learning convolutional neural networks; DWI, diffusion-weighted imaging; PET, positron emission tomography; RPV, radiomic prognostic vector; HR, hazard ratio; OS, overall survival; TCGA, The Cancer Genome Atlas; PFS, progression-free survival; CI, confidence interval.

based on the pathological findings. The traditional pathological diagnostic method is to stain the tissue with hematoxylin and eosin (H&E) and observe samples under a microscope (93). However, the method of diagnosis depends on the experience of the pathologists and is thus subjective. Furthermore, the storage of slices is a difficult problem after pathological diagnosis, and there are certain limitations in remote consultation. Whole slide imaging (WSI) can transform pathological tissue sections into high-resolution digital images using a computer and full-slice digital scanning technology. WSI has solved the limitations of traditional diagnostic methods, and has improved the efficiency and accuracy of pathological diagnosis (94). DL has been widely used in the field of medical pathological image recognition, where it can improve the degree of digitization of pathology and also plays a vital role in the analysis of pathological images (95).

Prediction of different pathological subtypes. The therapeutic scheme of OC is dependent on its pathological subtypes, which require different chemotherapy drugs and treatment plans. The identification of the subtypes predominantly relies on the subjective judgment of pathologists; however, the interobserver consistency of pathologists is often low (Cohen's κ , 0.54-0.67) (96). Farahani *et al* (96) developed four deep CNN algorithms to identify pathological subtypes of OC using WSI in 545 patients. The highest scoring CNN model showed high concordance with pathologists in diagnosing OC pathological subtypes [81.38% concordance (Cohen's κ , 0.7378) in the training set and 80.97% concordance (Cohen's κ , 0.7547) in the external dataset], indicating that CNN may be used as an auxiliary diagnostic model to improve the efficiency of diagnosing OC pathological subtypes. In addition, the model established based on WSI had good efficacy in predicting the effect of OC chemotherapy drugs. Wang *et al* (97) developed a weakly supervised DL to accurately predict the therapeutic effect of bevacizumab in patients with OC by analyzing the entire image of histological H&E staining. This method can guide clinical treatment decisions by screening out patients who are likely to show a poor response. A Cox proportional risk model showed that the model could predict patients at a higher risk of recurrence due to a poor treatment response compared with patients with a more favorable treatment response. The aforementioned results indicated that the combination of WSI and DL in pathology could effectively extract relevant information from high-throughput pathological data, and provide more instructive information for improved precision treatment.

Prediction of the mutation status of a gene. Different pathological types of EOCs exhibit varying gene mutation sites, with ~50% of EOCs displaying homologous recombination repair defects. Homologous recombination repair defects are primarily caused by mutations in the BRCA gene, which plays a crucial role in the DNA double-strand break repair process during homologous recombination repair and is considered an important tumor suppressor gene (66). Patients with advanced OC carrying BRCA1/2 mutations demonstrate increased sensitivity to platinum-based chemotherapy drugs, and exhibit higher objective remission rate and survival rates following treatment with platinum-based drugs. Furthermore, the use of poly(ADP-ribose) polymerase inhibitors after platinum-based

chemotherapy can significantly reduce the recurrence rate and the mortality rate of patients with OC (69). Notably, a DL model can be employed to identify gene mutations by analyzing the H&E-stained pathological images of tumors. Ho *et al* (98) utilized DL to analyze the WSI of patients with OC and developed a model that could predict the mutation status of the BRCA gene mutation in HGSOC. These studies demonstrate the potential of DL based on WSI in quantifying tumor histopathological features and related gene behavior. Nero *et al* (99) applied weakly supervised learning based on DL to analyze the WSI images of 66 patients with HGSOC. While the model exhibited zero errors in the training set, its performance in the verification set was mediocre, with an AUC of 0.59. In addition, this model was also used to predict PFS, with an AUC of 0.71, indicating a good prognostic performance.

Predict the efficacy and prognosis of drug therapy. Currently, the standard treatment for EOC is cytoreductive surgery combined with platinum-based chemotherapy, but patients with different pathological types of OC have different sensitivity levels to platinum-based chemotherapy. Laury *et al* (100) utilized the WSI of patients with HGSOC who underwent platinum-based chemotherapy with different resultant effects in order to establish a CNN model for predicting the effect of platinum-based chemotherapy. The CNN-based model was effective in distinguishing patients with different responses to platinum-based drugs, exhibiting both high sensitivity (73%) and specificity (91%). With the occurrence of chemotherapy resistance and refractory diseases, the sensitivity of platinum-based chemotherapy has declined (101). Bevacizumab, an antibody against vascular endothelial growth factor, has been used in the first- and second-line treatments of OC. Wang *et al* (102) collected the WSI results of patients with EOC and peritoneal serous papillary carcinoma, and established a DL model to predict the therapeutic effect of bevacizumab. The results showed that the new model could predict the effects of treatment without guidance or prior knowledge of the pathology. The proposed DL model could effectively distinguish patients who would respond well from the patients whose recurrence rate would be low after treatment and those whose disease was likely to deteriorate after treatment. Wu *et al* (103) appraised the WSI results of patients with OC through DL, and developed risk scores for these patients. The AUC of the time-dependent ROC curve verified the good predictive performance of risk scores. Additionally, the researchers analyzed the differential survival rate of patients with different homologous repair deficiency states using the aforementioned model. The DL model not only facilitated overall risk stratification of patients with OC, but also distinguished between different subtypes in terms of the prognosis, which could be used to provide a basis for targeted therapy for patients with OC (Table II).

4. Other AI-based omics in OC

Genomics. DL models based on various other omics-based approaches have also emerged in addition to radiography and pathological images, and these may also play a role in exploring the occurrence and development of diseases. Guo *et al* (104) applied DL to analyze multi-omics OC data using three datasets from the Gene Expression Omnibus

Table II. Overview of the studies on AI in WSI.

| A, Prediction of different pathological subtypes | | | | | |
|---|---------|--------------------|----------|--|--|
| First author, year | Disease | Number of patients | AI model | Main result | Main conclusion (Refs.) |
| Farahani <i>et al</i> , 2022 | OC | 545 | ML | The best-performing model achieved a diagnostic concordance of 81.38% (Cohen's κ , 0.7378) in the training set and 80.97% concordance (Cohen's κ , 0.7547) in the external dataset. | The CNN model may improve the diagnostic efficiency for determining OC pathological subtypes. (96) |
| Wang <i>et al</i> , 2022 | OC | 288 | DL | For an independent testing set, the three proposed methods obtained promising results with high recall (sensitivity) values of 0.946, 0.893 and 0.964, respectively. | The DL method can help identify patients with different treatment responses. (97) |
| B, Predict the mutation status of a gene | | | | | |
| First author, year | Disease | Number of patients | AI model | Main result | Main conclusion (Refs.) |
| Ho <i>et al</i> , 2023 | OC | 609 | DL | The model achieved an intersection-over-union value of 0.74, a recall value of 0.86 and a precision value of 0.84. | The DL model can be used to diagnose OC and find novel morphological patterns to predict molecular subtypes. (98) |
| Nero <i>et al</i> , 2022 | HGSOC | 644 | DL | The model achieved an AUC of 0.71, with a negative predictive value of 0.69 and a positive predictive value of 0.75 when applied to predict PFS. | The DL model based on WSI can predict BRCA1/2 gene status. (99) |
| C, Predict the efficacy and prognosis of drug therapy | | | | | |
| First author, year | Disease | Number of patients | AI model | Main result | Main conclusion (Refs.) |
| Laury <i>et al</i> , 2021 | HGSOC | 30 | CNN | The CNN model based on WSI discriminated the response to primary platinum-based chemotherapy with high sensitivity (73%) and specificity (91%). | DL based image analysis is able to predict outcome. (100) |
| Wang <i>et al</i> , 2022 | EOC | 720 | DL | The model in combination with AIM2 achieves high accuracy (0.92), recall (0.97), F-measure (0.93) and AUC (0.97) values for the first experiment (66% training and 34% testing) and high accuracy (0.86 \pm 0.07), precision (0.9 \pm 0.07), recall (0.85 \pm 0.06), F-measure (0.87 \pm 0.06) and AUC (0.91 \pm 0.05) for the second experiment using five-fold cross validation, respectively. | AIM2-DL model can distinguish patients gaining positive therapeutic effects with low cancer recurrence from patients with disease progression after treatment. (102) |

C, Predict the efficacy and prognosis of drug therapy

AI, artificial intelligence; OC, epithelial ovarian cancer; HGSOC, high-grade serous ovarian cancer; ML, machine learning; CNN, convolutional neural network; AUC, area under the curve; PFS, progression-free survival; WSI, whole slide imaging.

Metabolomics. Irajizad *et al* (110) performed metabolomic analysis on the serum samples from 101 patients with serous and non-serous OC, and 134 patients with benign pelvic masses. A total of seven cancer-related metabolites were screened using DL. The performance of DL for OC diagnosis in the early stage was significantly improved when combined with the risk of ovarian malignancy algorithm.

Thus far, AI-based radiomics has shown satisfactory efficiency in the diagnosis, differentiation and prognostic prediction of

OC. At the same time, the combination of AI models and traditional diagnoses from clinicians can improve the accuracy and efficiency of diagnosis, and may improve diagnostic systems in the future. In addition, the prediction of pathological typing and gene status may serve as a type of ‘virtual biopsy’, which could reduce the need for invasive tests on patients in the future. However, there remain several challenges in the clinical application of AI in OC. Firstly, while there are an increasing number of multi-omics studies based on genomics, transcriptomics and proteomics, there are fewer multi-omics studies combining radiomics and pathomics, which to some extent limits the clinical application of AI. The integration of multi-omics data has the potential to improve patient survival and facilitate future precision medicine approaches. Secondly, there are several AI algorithms, and current research only builds models around one or a few algorithms. It is necessary to conduct a multi-center comparison of these models to select the best AI models for general clinical application, so this scientific research can be truly implemented in a clinical setting. The number of clinical samples collected by general research institutes is small and often imbalanced in terms of representativeness of the subsequent feature extraction, which is a challenge for AI data processing. In future studies, considerably larger cohorts from multiple centers and indeed cohorts from multiple countries are needed to increase the validity of any models. Additionally, it is necessary to continuously innovate and improve the algorithms to optimize existing models. Finally, the clinical applications based on AI models are mostly concentrated in thyroid diseases, breast diseases and liver diseases, and the research of other systems remains predominantly in the theoretical stage. In future work, these clinical models should be used in clinical prospective studies to assist clinicians in diagnostic and prognostic analyses. The problems and effects encountered by clinicians when applying artificial intelligence models should then be summarized, and the models constantly optimized. Advances in AI-based approaches will improve diagnostic accuracy, accelerate the diagnostic process, and play a key role in assisting doctors in decision-making and intelligent monitoring in the future.

In conclusion, AI has emerged as a powerful tool for the processing of large datasets, and is being extensively utilized in the development of diverse omics models for OC. Multi-omics analysis, including imaging, pathomics, genomics, metabolomics and proteomics, has demonstrated potential in enhancing the accuracy of OC diagnoses, the differentiation between benign and malignant cases, and the prediction of pathological types and prognosis. The integration of multi-omics data has the potential to improve patient survival and facilitate precision medicine in the future.

Acknowledgements

Not applicable.

Funding

This study was funded by the Special Fund for Doctoral Supervisors of The Second Affiliated Hospital of Fujian Medical University (grant no. 2022BD1005).

Availability of data and materials

Not applicable.

Authors' contributions

YW, WL, GL and LL conceived and designed the article. YW contributed to collecting data and editing the manuscript. WL and XW contributed to researching the literature, and revising the content with regard to obstetrics and gynecology. XZ and YH contributed to revising the content with regard to pathology. GL gave final approval of the manuscript. All authors have read and approved the final version of the manuscript. The authors guarantee that no AI tools were used to produce any content in the article. Data authentication is not applicable.

Ethics approval and consent to participate

Not applicable.

Patient consent for publication

Not applicable.

Competing interests

The authors declare that they have no competing interests.

References

1. Siegel RL, Miller KD, Wagle NS and Jemal A: Cancer statistics, 2023. *CA Cancer J Clin* 73: 17-48, 2023.
2. Sung H, Ferlay J, Siegel RL, Laversanne M, Soerjomataram I, Jemal A and Bray F: Global cancer statistics 2020: GLOBOCAN estimates of incidence and mortality worldwide for 36 cancers in 185 countries. *CA Cancer J Clin* 71: 209-249, 2021.
3. Allemani C, Weir HK, Carreira H, Harewood R, Spika D, Wang XS, Bannon F, Ahn JV, Johnson CJ, Bonaventure A, *et al*: Global surveillance of cancer survival 1995-2009: Analysis of individual data for 25,676,887 patients from 279 population-based registries in 67 countries (CONCORD-2). *Lancet* 385: 977-1010, 2015.
4. Millstein J, Budden T, Goode EL, Anglesio MS, Talhouk A, Intermaggio MP, Leong HS, Chen S, Elatre W, Gilks B, *et al*: Prognostic gene expression signature for high-grade serous ovarian cancer. *Ann Oncol* 31: 1240-1250, 2020.
5. Kurman RJ and Shih IM: The origin and pathogenesis of epithelial ovarian cancer: A proposed unifying theory. *Am J Surg Pathol* 34: 433-443, 2010.
6. Schmeler KM, Tao X, Frumovitz M, Deavers MT, Sun CC, Sood AK, Brown J, Gershenson DM and Ramirez PT: Prevalence of lymph node metastasis in primary mucinous carcinoma of the ovary. *Obstet Gynecol* 116: 269-273, 2010.
7. Wang KH and Ding DC: The role and applications of exosomes in gynecological cancer: A review. *Cell Transplant* 32: 9636897231195240, 2023.
8. Khella CA, Mehta GA, Mehta RN and Gatz ML: Recent advances in integrative multi-omics research in breast and ovarian cancer. *J Pers Med* 11: 149, 2021.
9. Yu H, Wang J, Wu B, Li J and Chen R: Prognostic significance and risk factors for pelvic and para-aortic lymph node metastasis in type I and type II ovarian cancer: A large population-based database analysis. *J Ovarian Res* 16: 28, 2023.
10. Chang YH, Wu KC, Harnod T and Ding DC: The organoid: A research model for ovarian cancer. *Tzu Chi Med J* 34: 255-260, 2022.
11. Kurman RJ and Shih IM: The dualistic model of ovarian carcinogenesis: Revisited, revised, and expanded. *Am J Pathol* 186: 733-747, 2016.

12. Zhang T, Liu Q, Zhu Y, Huang Y, Qin J, Wu X and Zhang S: Lymphocyte and macrophage infiltration in omental metastases indicates poor prognosis in advance stage epithelial ovarian cancer. *J Int Med Res* 49: 3000605211066245, 2021.
13. Shrestha P, Poudyal B, Yadollahi S, Wrigh DE, Gregor AV, Warne JD, Korfiati P, Gree IC, Rassie KL, Mariani A, *et al*: A systematic review on the use of artificial intelligence in gynecologic imaging-Background, state of the art, and future directions. *Gynecol Oncol* 166: 596-605, 2022.
14. Mikdadi D, O'Connell KA, Meacham PJ, Dugan MA, Ojieri MO, Carlson TB and Klenk JA: Applications of artificial intelligence (AI) in ovarian cancer, pancreatic cancer, and image biomarker discovery. *Cancer Biomark* 33: 173-184, 2022.
15. Breen J, Allen K, Zucker K, Adusumilli P, Scarsbrook A, Hall G, Orsi NM and Ravikumar N: Artificial intelligence in ovarian cancer histopathology: A systematic review. *NPJ Precis Oncol* 7: 83, 2023.
16. Lambin P, Rios-Velazquez E, Leijenaar R, Carvalho S, van Stiphout RG, Granton P, Zegers CM, Gillies R, Boellard R, Dekker A and Aerts HJ: Radiomics: Extracting more information from medical images using advanced feature analysis. *Eur J Cancer* 48: 441-446, 2012.
17. Tagliafico AS, Piana M, Schenone D, Lai R, Massone AM and Houssami N: Overview of radiomics in breast cancer diagnosis and prognostication. *Breast* 49: 74-80, 2020.
18. Aerts HJ, Velazquez ER, Leijenaar RT, Parmar C, Grossmann P, Carvalho S, Bussink J, Monshouwer R, Haibe-Kains B, Rietveld D, *et al*: Decoding tumour phenotype by noninvasive imaging using a quantitative radiomics approach. *Nat Commun* 5: 4006, 2014.
19. Sun R, Orlhac F, Robert C, Reuzé S, Schernberg A, Buvat I, Deutsch E and Fertet C: In regard to mattonen et al. *Int J Radiat Oncol Biol Phys* 95: 1544-1545, 2016.
20. Tong Y, Zhang J, Wei Y, Yu J, Zhan W, Xia H, Zhou S, Wang Y and Chang C: Ultrasound-based radiomics analysis for preoperative prediction of central and lateral cervical lymph node metastasis in papillary thyroid carcinoma: A multi-institutional study. *BMC Med Imaging* 22: 82, 2022.
21. Du Y, Zha HL, Wang H, Liu XP, Pan JZ, Du LW, Cai MJ, Zong M and Li CY: Ultrasound-based radiomics nomogram for differentiation of triple-negative breast cancer from fibroadenoma. *Br J Radiol* 95: 20210598, 2022.
22. Peng Y, Lin P, Wu L, Wan D, Zhao Y, Liang L, Ma X, Qin H, Liu Y, Li X, *et al*: Ultrasound-Based radiomics analysis for preoperatively predicting different histopathological subtypes of primary liver cancer. *Front Oncol* 10: 1646, 2020.
23. Ou W, Lei J, Li M, Zhang X, Liang R, Long L, Wang C, Chen L, Chen J, Zhang J and Wang Z: Ultrasound-based radiomics score for pre-biopsy prediction of prostate cancer to reduce unnecessary biopsies. *Prostate* 83: 109-118, 2023.
24. Avesani G, Tran HE, Cammarata G, Botta F, Raimondi S, Russo L, Persiani S, Bonatti M, Tagliaferri T, Dolciami M, *et al*: CT-based radiomics and deep learning for BRCA mutation and progression-free survival prediction in ovarian cancer using a multicentric dataset. *Cancers (Basel)* 14: 2379, 2022.
25. Levy MA, Freymann JB, Kirby JS, Fedorov A, Fennessy FM, Eschrich SA, Berglund AE, Fenstermacher DA, Tan Y, Guo X, *et al*: Informatics methods to enable sharing of quantitative imaging research data. *Magn Reson Imaging* 30: 1249-1256, 2012.
26. Beer L, Martin-Gonzalez P, Delgado-Ortíz M, Reinis M, Rundo L, Woitek R, Ursprung S, Escudero L, Sahin H, Funingana IG, *et al*: Ultrasound-guided targeted biopsies of CT-based radiomic tumour habitats: Technical development and initial experience in metastatic ovarian cancer. *Eur Radiol* 31: 3765-3772, 2021.
27. Karimi D, Dou H, Warfield SK and Gholipour A: Deep learning with noisy labels: Exploring techniques and remedies in medical image analysis. *Med Image Anal* 65: 101759, 2020.
28. Kumar V, Gu Y, Basu S, Berglund A, Eschrich SA, Schabath MB, Forster K, Aerts HJ, Dekker A, Fenstermacher D, *et al*: Radiomics: The process and the challenges. *Magn Reson Imaging* 30: 1234-1248, 2012.
29. Peeken JC, Bernhofer M, Wiessler B, Goldberg T, Cremers D, Rost B, Wilkens JJ, Combs SE and Nüsslin F: Radiomics in radiooncology-challenging the medical physicist. *Phys Med* 48: 27-36, 2018.
30. Koh YW, Lee D and Lee SJ: Intratumoral heterogeneity as measured using the tumor-stroma ratio and PET texture analyses in females with lung adenocarcinomas differs from that of males with lung adenocarcinomas or squamous cell carcinomas. *Medicine (Baltimore)* 98: e14876, 2019.
31. Busnatu Ș, Niculescu AG, Bolocan A, Petrescu GED, Păduraru DN, Năstăsă I, Lupușoru M, Geantă M, Andronic O, Grumezescu AM and Martins H: Clinical applications of artificial intelligence-an updated overview. *J Clin Med* 11: 2265, 2022.
32. Oakden-Rayner L, Carneiro G, Bessen T, Nascimento JC, Bradley AP and Palmer LJ: Precision radiology: Predicting longevity using feature engineering and deep learning methods in a radiomics framework. *Sci Rep* 7: 1648, 2017.
33. Li W, Dong S, Wang H, Wu R, Wu H, Tang ZR, Zhang J, Hu Z and Yin C: Risk analysis of pulmonary metastasis of chondrosarcoma by establishing and validating a new clinical prediction model: A clinical study based on SEER database. *BMC Musculoskelet Disord* 22: 529, 2021.
34. Chen L, Zeng H, Xiang Y, Huang Y, Luo Y and Ma X: Histopathological images and multi-omics integration predict molecular characteristics and survival in lung adenocarcinoma. *Front Cell Dev Biol* 9: 720110, 2021.
35. Guo S, Tian M, Fan Y and Zhang X: Recent advances in mass spectrometry-based proteomics and metabolomics in chronic rhinosinusitis with nasal polyps. *Front Immunol* 14: 1267194, 2023.
36. Zeng H, Chen L, Zhang M, Luo Y and Ma X: Integration of histopathological images and multi-dimensional omics analyses predicts molecular features and prognosis in high-grade serous ovarian cancer. *Gynecol Oncol* 163: 171-180, 2021.
37. Gupta L, Srivastava D, Sahu M, Tiwari S, Ambasta RK and Kumar P: Artificial intelligence to deep learning: Machine intelligence approach for drug discovery. *Mol Divers* 25: 1315-1360, 2021.
38. European Society of Radiology (ESR): What the radiologist should know about artificial intelligence-an ESR white paper. *Insights Imaging* 10: 44, 2019.
39. Joda T, Bornstein MM, Jung RE, Ferrari M, Waltimo T and Zitzmann NU: Recent trends and future direction of dental research in the digital era. *Int J Environ Res Public Health* 17: 1987, 2020.
40. Covas P, De Guzman E, Barrows I, Bradley AJ, Choi BG, Krepp JM, Lewis JF, Katz R, Tracy CM, Zeman RK, *et al*: Artificial intelligence advancements in the cardiovascular imaging of coronary atherosclerosis. *Front Cardiovasc Med* 9: 839400, 2022.
41. Li W, Dong Y, Liu W, Tang Z, Sun C, Lowe S, Chen S, Bentley R, Zhou Q, Xu C, *et al*: A deep belief network-based clinical decision system for patients with osteosarcoma. *Front Immunol* 13: 1003347, 2022.
42. Chen L, Han Z, Wang J and Yang C: The emerging roles of machine learning in cardiovascular diseases: A narrative review. *Ann Transl Med* 10: 611, 2022.
43. Zhao J, Luo Y, Xiao R, Wu R and Fan T: Tri-training algorithm for adaptive nearest neighbor density editing and cross entropy evaluation. *Entropy (Basel)* 25: 480, 2023.
44. Awassa L, Jdey I, Dhahri H, Hcini G, Mahmood A, Othman E and Haneef M: Study of different deep learning methods for coronavirus (COVID-19) pandemic: Taxonomy, survey and insights. *Sensors (Basel)* 22: 1890, 2022.
45. Zhang Z, Zhu Y, Liu M, Zhang Z, Zhao Y, Yang X, Xie M and Zhang L: Artificial intelligence-enhanced echocardiography for systolic function assessment. *J Clin Med* 11: 2893, 2022.
46. Chen S, Zhao S and Lan Q: Residual block based nested U-type architecture for multi-modal brain tumor image segmentation. *Front Neurosci* 16: 832824, 2022.
47. Park CW, Oh SJ, Kim KS, Jang MC, Kim IS, Lee YK, Chung MJ, Cho BH and Seo SW: Artificial intelligence-based classification of bone tumors in the proximal femur on plain radiographs: System development and validation. *PLoS One* 17: e0264140, 2022.
48. Wu W, Huang Y and Wu X: A new deep learning method with self-supervised learning for delineation of the electrocardiogram. *Entropy (Basel)* 24: 1828, 2022.
49. Kaka H, Zhang E and Khan N: Artificial intelligence and deep learning in neuroradiology: Exploring the new frontier. *Can Assoc Radiol J* 72: 35-44, 2021.
50. Liu P, Liang X, Liao S and Lu Z: Pattern classification for ovarian tumors by integration of radiomics and deep learning features. *Curr Med Imaging* 18: 1486-1502, 2022.
51. Qin X, Hu X, Xiao W, Zhu C, Ma Q and Zhang C: Preoperative evaluation of hepatocellular carcinoma differentiation using contrast-enhanced ultrasound-based deep-learning radiomics model. *J Hepatocell Carcinoma* 10: 157-168, 2023.
52. Wang M, Peruchio JAU, Hu Y, Choi MH, Han L, Wong EMF, Ho G, Zhang X, Ip P and Lee EYP: Computed tomographic radiomics in differentiating histologic subtypes of epithelial ovarian carcinoma. *JAMA Netw Open* 5: e2245141, 2022.

53. Li S, Liu J, Xiong Y, Pang P, Lei P, Zou H, Zhang M, Fan B and Luo P: A radiomics approach for automated diagnosis of ovarian neoplasm malignancy in computed tomography. *Sci Rep* 11: 8730, 2021.
54. Saida T, Mori K, Hoshiai S, Sakai M, Urushibara A, Ishiguro T, Minami M, Satoh T and Nakajima T: Diagnosing ovarian cancer on MRI: A preliminary study comparing deep learning and radiologist assessments. *Cancers (Basel)* 14: 987, 2022.
55. Gao Y, Zeng S, Xu X, Li H, Yao S, Song K, Li X, Chen L, Tang J, Xing H, *et al*: Deep learning-enabled pelvic ultrasound images for accurate diagnosis of ovarian cancer in China: A retrospective, multicentre, diagnostic study. *Lancet Digit Health* 4: e179-e187, 2022.
56. Wang Y, Zhang H, Wang T, Yao L, Zhang G, Liu X, Yang G and Yuan L: Deep learning for the ovarian lesion localization and discrimination between borderline and malignant ovarian tumors based on routine MR imaging. *Sci Rep* 13: 2770, 2023.
57. Andreotti RF, Timmerman D, Strachowski LM, Froyman W, Benacerraf BR, Bennett GL, Bourne T, Brown DL, Coleman BG, Frates MC, *et al*: O-RADS US risk stratification and management system: A consensus guideline from the ACR ovarian-adnexal reporting and data system committee. *Radiology* 294: 168-185, 2020.
58. Chen H, Yang BW, Qian L, Meng YS, Bai XH, Hong XW, He X, Jiang MJ, Yuan F, Du QW and Feng WW: Deep learning prediction of ovarian malignancy at US compared with O-RADS and expert assessment. *Radiology* 304: 106-113, 2022.
59. Jung Y, Kim T, Han MR, Kim S, Kim G, Lee S and Choi YJ: Ovarian tumor diagnosis using deep convolutional neural networks and a denoising convolutional autoencoder. *Sci Rep* 12: 17024, 2022.
60. Christiansen F, Epstein EL, Smedberg E, Åkerlund M, Smith K and Epstein E: Ultrasound image analysis using deep neural networks for discriminating between benign and malignant ovarian tumors: Comparison with expert subjective assessment. *Ultrasound Obstet Gynecol* 57: 155-163, 2021.
61. Harris HR, Guertin KA, Camacho TF, Johnson CE, Wu AH, Moorman PG, Myers E, Bethea TN, Bandera EV, Joslin CE, *et al*: Racial disparities in epithelial ovarian cancer survival: An examination of contributing factors in the ovarian cancer in women of African Ancestry consortium. *Int J Cancer* 151: 1228-1239, 2022.
62. Tang ZP, Ma Z, He Y, Liu RC, Jin BB, Wen DY, Wen R, Yin HH, Qiu CC, Gao RZ, *et al*: Ultrasound-based radiomics for predicting different pathological subtypes of epithelial ovarian cancer before surgery. *BMC Med Imaging* 22: 147, 2022.
63. Xu Y, Luo HJ, Ren J, Guo LM, Niu J and Song X: Diffusion-weighted imaging-based radiomics in epithelial ovarian tumors: Assessment of histologic subtype. *Front Oncol* 12: 978123, 2022.
64. Jian J, Li Y, Pickhardt PJ, Xia W, He Z, Zhang R, Zhao S, Zhao X, Cai S, Zhang J, *et al*: MR image-based radiomics to differentiate type I and type II epithelial ovarian cancers. *Eur Radiol* 31: 403-410, 2021.
65. Konstantinopoulos PA, Ceccaldi R, Shapiro GI and D'Andrea AD: Homologous recombination deficiency: Exploiting the fundamental vulnerability of ovarian cancer. *Cancer Discov* 5: 1137-1154, 2015.
66. Tutt A, Tovey H, Cheang MCU, Kernaghan S, Kilburn L, Gazinska P, Owen J, Abraham J, Barrett S, Barrett-Lee P, *et al*: Carboplatin in BRCA1/2-mutated and triple-negative breast cancer BRCAness subgroups: The TNT trial. *Nat Med* 24: 628-637, 2018.
67. Golan T, Sella T, O'Reilly EM, Katz MH, Epelbaum R, Kelsen DP, Borgida A, Maynard H, Kindler H, Friedmen E, *et al*: Overall survival and clinical characteristics of BRCA mutation carriers with stage I/II pancreatic cancer. *Br J Cancer* 116: 697-702, 2017.
68. Li MR, Liu MZ, Ge YQ, Zhou Y and Wei W: Assistance by routine CT features combined with 3D texture analysis in the diagnosis of BRCA gene mutation status in advanced epithelial ovarian cancer. *Front Oncol* 11: 696780, 2021.
69. Moore K, Colombo N, Scambia G, Kim BG, Oaknin A, Friedlander M, Lisysanskaya A, Floquet A, Leary A, Sonke GS, *et al*: Maintenance olaparib in patients with newly diagnosed advanced ovarian cancer. *N Engl J Med* 379: 2495-2505, 2018.
70. Soslow RA, Han G, Park KJ, Garg K, Olvera N, Spriggs DR, Kauff ND and Levine DA: Morphologic patterns associated with BRCA1 and BRCA2 genotype in ovarian carcinoma. *Mod Pathol* 25: 625-636, 2012.
71. Alsop K, Fereday S, Meldrum C, deFazio A, Emmanuel C, George J, Dobrovic A, Birrer MJ, Webb PM, Stewart C, *et al*: BRCA mutation frequency and patterns of treatment response in BRCA mutation-positive women with ovarian cancer: A report from the Australian ovarian cancer study group. *J Clin Oncol* 30: 2654-2663, 2012.
72. Sánchez-Lorenzo L, Salas-Benito D, Villamayor J, Patiño-García A and González-Martín A: The BRCA gene in epithelial ovarian cancer. *Cancers (Basel)* 14: 1235, 2022.
73. Meier A, Veeraraghavan H, Nougaret S, Lakhman Y, Sosa R, Soslow RA, Sutton EJ, Hricak H, Sala E and Vargas HA: Association between CT-texture-derived tumor heterogeneity, outcomes, and BRCA mutation status in patients with high-grade serous ovarian cancer. *Abdom Radiol (NY)* 44: 2040-2047, 2019.
74. Verhaak RG, Tamayo P, Yang JY, Hubbard D, Zhang H, Creighton CJ, Fereday S, Lawrence M, Carter SL, Mermel CH, *et al*: Prognostically relevant gene signatures of high-grade serous ovarian carcinoma. *J Clin Invest* 123: 517-525, 2013.
75. Vargas HA, Huang EP, Lakhman Y, Ippolito JE, Bhosale P, Mellnick V, Shinagare AB, Anello M, Kirby J, Fevrier-Sullivan B, *et al*: Radiogenomics of high-grade serous ovarian cancer: Multireader multi-institutional study from the cancer genome atlas ovarian cancer imaging research group. *Radiology* 285: 482-492, 2017.
76. Wang X, Xu C, Grzegorzek M and Sun H: Habitat radiomics analysis of pet/ct imaging in high-grade serous ovarian cancer: Application to Ki-67 status and progression-free survival. *Front Physiol* 13: 948767, 2022.
77. Heintz AP, Odicino F, Maisonneuve P, Quinn MA, Benedet JL, Creasman WT, Ngan HY, Pecorelli S and Beller U: Carcinoma of the ovary. FIGO 26th annual report on the results of treatment in gynecological cancer. *Int J Gynaecol Obstet* 95 (Suppl 1): S161-S192, 2006.
78. Suidan RS, Ramirez PT, Sarasohn DM, Teitcher JB, Mironov S, Iyer RB, Zhou Q, Iasonos A, Paul H, Hosaka M, *et al*: A multicenter prospective trial evaluating the ability of preoperative computed tomography scan and serum CA-125 to predict suboptimal cytoreduction at primary debulking surgery for advanced ovarian, fallopian tube, and peritoneal cancer. *Gynecol Oncol* 134: 455-461, 2014.
79. Peng Z, Lin Z, He A, Yi L, Jin M, Chen Z, Tao Y, Yang Y, Cui C, Liu Y and Zuo M: Development and validation of a comprehensive model for predicting distant metastasis of solid lung adenocarcinoma: 3D radiomics, 2D radiomics and clinical features. *Cancer Manag Res* 14: 3437-3448, 2022.
80. Ai Y, Zhang J, Jin J, Zhang J, Zhu H and Jin X: Preoperative prediction of metastasis for ovarian cancer based on computed tomography radiomics features and clinical factors. *Front Oncol* 11: 610742, 2021.
81. Yu XY, Ren J, Jia Y, Wu H, Niu G, Liu A, Gao Y, Hao F and Xie L: Multiparameter MRI radiomics model predicts preoperative peritoneal carcinomatosis in ovarian cancer. *Front Oncol* 11: 765652, 2021.
82. Chien J and Poole EM: Ovarian cancer prevention, screening, and early detection: Report from the 11th biennial ovarian cancer research symposium. *Int J Gynecol Cancer* 27: S20-S22, 2017.
83. Yang R, Niepel M, Mitchison TK and Sorger PK: Dissecting variability in responses to cancer chemotherapy through systems pharmacology. *Clin Pharmacol Ther* 88: 34-38, 2010.
84. Luvero D, Milani A and Ledermann JA: Treatment options in recurrent ovarian cancer: Latest evidence and clinical potential. *Ther Adv Med Oncol* 6: 229-239, 2014.
85. Lu H, Arshad M, Thornton A, Avesani G, Cunnea P, Curry E, Kanavati F, Liang J, Nixon K, Williams ST, *et al*: A mathematical-descriptor of tumor-mesoscopic-structure from computed-tomography images annotates prognostic- and molecular-phenotypes of epithelial ovarian cancer. *Nat Commun* 10: 764, 2019.
86. Hong Y, Liu Z, Lin D, Peng J, Yuan Q, Zeng Y, Wang X and Luo C: Development of a radiomic-clinical nomogram for prediction of survival in patients with serous ovarian cancer. *Clin Radiol* 77: 352-359, 2022.
87. Wei W, Liu Z, Rong Y, Zhou B, Bai Y, Wei W, Wang S, Wang M, Guo Y and Tian J: A computed tomography-based radiomic prognostic marker of advanced high-grade serous ovarian cancer recurrence: A multicenter study. *Front Oncol* 9: 255, 2019.
88. Wang S, Liu Z, Rong Y, Zhou B, Bai Y, Wei W, Wang M, Guo Y and Tian J: Deep learning provides a new computed tomography-based prognostic biomarker for recurrence prediction in high-grade serous ovarian cancer. *Radiation Oncol* 132: 171-177, 2019.

89. Liu L, Wan H, Liu L, Wang J, Tang Y, Cui S and Li Y: Deep learning provides a new magnetic resonance imaging-based prognostic biomarker for recurrence prediction in high-grade serous ovarian cancer. *Diagnostics (Basel)* 13: 748, 2023.
90. Yao F, Ding J, Hu Z, Cai M, Liu J, Huang X, Zheng R, Lin F and Lan L: Ultrasound-based radiomics score: A potential biomarker for the prediction of progression-free survival in ovarian epithelial cancer. *Abdom Radiol (NY)* 46: 4936-4945, 2021.
91. Laios A, De Freitas DLD, Saalmink G, Tan YS, Johnson R, Zubayraeva A, Munot S, Hutson R, Thangavelu A, Broadhead T, *et al*: Stratification of length of stay prediction following surgical cytoreduction in advanced high-grade serous ovarian cancer patients using artificial intelligence; the leeds L-AI-OS score. *Curr Oncol* 29: 9088-9104, 2022.
92. Lei R, Yu Y, Li Q, Ya Q, Wan J, Ga M, Zhuo W, Ren W, Ta Y, Zhan B, *et al*: Deep learning magnetic resonance imaging predicts platinum sensitivity in patients with epithelial ovarian cancer. *Front Oncol* 12: 895177, 2022.
93. Fereidouni F and Levenson R: Beyond brightfield: A possible future of slide scanners. *Biotechniques* 70: 5-6, 2021.
94. Boehm KM, Aherne EA, Ellenson L, Nikolovski I, Alghamdi M, Vázquez-García I, Zamarrin D, Roche KL, Liu Y, Patel D, *et al*: Multimodal data integration using machine learning improves risk stratification of high-grade serous ovarian cancer. *Nat Cancer* 3: 723-733, 2022.
95. Jiang Z, Song L, Lu H and Yin J: The potential use of DCE-MRI texture analysis to predict HER2 2+ status. *Front Oncol* 9: 242, 2019.
96. Farahani H, Boschman J, Farnell D, Darbandsari A, Zhang A, Ahmadvand P, Jones SJM, Huntsman D, Köbel M, Gilks CB, *et al*: Deep learning-based histotype diagnosis of ovarian carcinoma whole-slide pathology images. *Mod Pathol* 35: 1983-1990, 2022.
97. Wang CW, Chang CC, Lee YC, Lin YJ, Lo SC, Hsu PC, Liou YA, Wang CH and Chao TK: Weakly supervised deep learning for prediction of treatment effectiveness on ovarian cancer from histopathology images. *Comput Med Imaging Graph* 99: 102093, 2022.
98. Ho DJ, Chui MH, Vanderbilt CM, Jung J, Robson ME, Park CS, Roh J and Fuchs TJ: Deep interactive learning-based ovarian cancer segmentation of H&E-stained whole slide images to study morphological patterns of BRCA mutation. *J Pathol Inform* 14: 100160, 2023.
99. Nero C, Boldrini L, Lenkowicz J, Giudice MT, Piermattei A, Inzani F, Pasciuto T, Minucci A, Fagotti A, Zannoni G, *et al*: Deep-learning to predict BRCA mutation and survival from digital H&E slides of epithelial ovarian cancer. *Int J Mol Sci* 23: 11326, 2022.
100. Laury AR, Blom S, Ropponen T, Virtanen A and Carpen OM: Artificial intelligence-based image analysis can predict outcome in high-grade serous carcinoma via histology alone. *Sci Rep* 11: 19165, 2021.
101. Lim HJ and Ledger W: Targeted therapy in ovarian cancer. *Womens Health (Lond)* 12: 363-378, 2016.
102. Wang CW, Lee YC, Chang CC, Lin YJ, Liou YA, Hsu PC, Chang CC, Sai AK, Wang CH and Chao TK: A weakly supervised deep learning method for guiding ovarian cancer treatment and identifying an effective biomarker. *Cancers (Basel)* 14: 1651, 2022.
103. Wu M, Zhu C, Yang J, Cheng S, Yang X, Gu S, Xu S, Wu Y, Shen W, Huang S and Wang Y: Exploring prognostic indicators in the pathological images of ovarian cancer based on a deep survival network. *Front Genet* 13: 1069673, 2022.
104. Guo LY, Wu AH, Wang YX, Zhang LP, Chai H and Liang XF: Deep learning-based ovarian cancer subtypes identification using multi-omics data. *BioData Min* 13: 10, 2020.
105. Ye L, Zhang Y, Yang X, Shen F and Xu B: An ovarian cancer susceptible gene prediction method based on deep learning methods. *Front Cell Dev Biol* 9: 730475, 2021.
106. Bahado-Singh RO, Ibrahim A, Al-Wahab Z, Aydas B, Radhakrishna U, Yilmaz A and Vishweswaraiah S: Precision gynecologic oncology: Circulating cell free DNA epigenomic analysis, artificial intelligence and the accurate detection of ovarian cancer. *Sci Rep* 12: 18625, 2022.
107. Aghayousefi R, Khatibi SM, Vahed SZ, Bastami M, Pirmoradi S and Teshnehlab M: A diagnostic miRNA panel to detect recurrence of ovarian cancer through artificial intelligence approaches. *J Cancer Res Clin Oncol* 149: 325-341, 2023.
108. Hamidi F, Gilani N, Belaghi RA, Sarbakhsh P, Edgünlü T and Santaguida P: Exploration of potential miRNA biomarkers and prediction for ovarian cancer using artificial intelligence. *Front Genet* 12: 724785, 2021.
109. Yokoi A, Matsuzaki J, Yamamoto Y, Yoneoka Y, Takahashi K, Shimizu H, Uehara T, Ishikawa M, Ikeda SI, Sonoda T, *et al*: Integrated extracellular microRNA profiling for ovarian cancer screening. *Nat Commun* 9: 4319, 2018.
110. Irajizad E, Han CY, Celestino J, Wu R, Murage E, Spencer R, Dennison JB, Vykoukal J, Long JP, Do KA, *et al*: A blood-based metabolite panel for distinguishing ovarian cancer from benign pelvic masses. *Clin Cancer Res* 28: 4669-4676, 2022.



Copyright © 2024 Wang et al. This work is licensed under a Creative Commons Attribution-NonCommercial-NoDerivatives 4.0 International (CC BY-NC-ND 4.0) License.